



Aqueous-phase hydrodeoxygenation of sorbitol with Pt/SiO₂–Al₂O₃: Identification of reaction intermediates

Ning Li, George W. Huber*

Department of Chemical Engineering, University of Massachusetts, 159 Goessmann Lab., 686 North Pleasant Street, Amherst, MA 01003-9303, USA

ARTICLE INFO

Article history:

Received 1 September 2009

Revised 4 December 2009

Accepted 5 December 2009

Available online 8 January 2010

Keywords:

Alkane production

Biofuels

Biomass conversion

Bifunctional catalysis

Pt

SiO₂–Al₂O₃

ABSTRACT

Aqueous-phase hydrodeoxygenation of sugar and sugar-derived molecules can be used to produce a range of alkanes and oxygenates. In this paper, we have identified the reaction intermediates and reaction chemistry for the aqueous-phase hydrodeoxygenation of sorbitol over a bifunctional catalyst (Pt/SiO₂–Al₂O₃) that contains both metal (Pt) and acid (SiO₂–Al₂O₃) sites. A wide variety of reactions occur in this process including C–C bond cleavage, C–O bond cleavage, and hydrogenation reactions. The key C–C bond cleavage reactions include: retro-aldol condensation and decarbonylation, which both occur on metal catalytic sites. Dehydration is the key C–O bond cleavage reaction and occurs on acid catalytic sites. Sorbitol initially undergoes dehydration and ring closure to produce cyclic C₆ molecules or retro-aldol condensation reactions to produce primarily C₃ polyols. Isosorbide is the major final product from sorbitol dehydration. Isosorbide then undergoes ring opening hydrogenation reactions and a dehydration/hydrogenation step to form 1,2,6-hexanetriol. The hexanetriol is then converted into hexanol and hexane by dehydration/hydrogenation. Smaller oxygenates are produced by C–C bond cleavage. These smaller oxygenates undergo dehydration/hydrogenation reactions to produce alkanes from C₁–C₅. The results from this paper suggest that hydrodeoxygenation chemistry can be tuned to make a wide variety of products from biomass-derived oxygenates.

© 2009 Elsevier Inc. All rights reserved.

1. Introduction

Declining fossil fuel reserves combined with increasing fossil fuel prices are making it imperative to develop new economical and energy-efficient process for the production of fuel from renewable resources. Plant biomass is the only renewable source of carbon that can be used to make liquid fuels and chemicals [1]. Selectively removing oxygen from the biomass-derived species is one of the key challenges with converting renewable biomass resources into fuels and chemicals. Aqueous phase processing (APP) [2,3] is a promising conversion option for the conversion of aqueous biomass-derived feedstocks (including sugars, sugar alcohols and bio-oils) into hydrogen [4–10], light alkanes (even gasoline) [8,11,12], liquid alkanes [13–18], and oxygenates [3,19–24]. Aqueous-phase hydrodeoxygenation (APHDO), a key process in APP, involves the conversion of oxygenated molecules into alkanes by a series of dehydration and hydrogenation step [11,14,15]. In APHDO process, the bifunctional catalysts containing metal (Pt and Pd) and acid (such as SiO₂–Al₂O₃ or mineral acid) sites were used. The oxygen is removed from the biomass with APHDO by a combination of C–C and C–O bond cleavage reaction. Once the oxygen is removed from the biomass, hydrogen is then added to

the oxygen-deficient molecules by hydrogenation on metal catalytic sites. A wide variety of products can be generated by hydrodeoxygenation reaction pathways. The products generated depend on the relative rates of C–C vs. C–O bond cleavage. If larger alkanes or oxygenates (i.e. C₅–C₆) are desired, then C–C bond cleavage should be inhibited and the rate of C–O bond cleavage should increase. If smaller alkanes and oxygenates are desired, then relative rate of C–C bond cleavage vs. C–O bond cleavage should be increased. While Dumesic and co-workers [11] have previously shown that APHDO to convert sorbitol into alkanes ranging from C₁ to C₆ alkanes, little is known about the reaction chemistry that occurs in this process. The reaction intermediates produced in this process are unknown. The exact nature of the C–C vs. C–O bond cleavage is also unknown.

The purpose of this paper is to understand the reaction chemistry and identify the key reaction intermediates that are produced in APHDO of sorbitol. In this paper, we have identified the key reaction intermediates and discussed how these intermediates could be selectively produced by adjusting the relative rates of C–C vs. C–O bond cleavage. We showed that the product selectivity can be adjusted by changing the relative rates of C–C vs. C–O bond cleavage. As we will show in this paper, C–C bond cleavage occurs over metal active sites by two major pathways retro-aldol condensation and decarbonylation. C–O bond cleavage happens on acid sites by dehydration reactions

* Corresponding author. Fax: +1 413 545 1647.

E-mail address: huber@ecs.umass.edu (G.W. Huber).

2. Experimental

2.1. Catalyst preparation

The Pt/SiO₂–Al₂O₃ catalyst used in this work was prepared by an incipient wetness impregnation of SiO₂–Al₂O₃ (SIAL3125, Grace Davison, SiO₂/Al₂O₃ molar ratio about 4.0) with tetra-amine platinum nitrate (Strem Chemicals) aqueous solution according to literature [11,15]. The Pt content in the catalyst was 4 weight% (wt.%). The mixture was then dried in an oven overnight at 373 K and calcinated at 533 K for 3 h in air.

2.2. Catalyst characterization

XRD patterns of the 4 wt.% Pt/SiO₂–Al₂O₃ as prepared were obtained with a Philips XPERT powder diffractometer equipped with an on-line computer. The Ni-filtered Cu K α radiation was used. The specific surface area of the catalyst was determined by nitrogen adsorption at 77 K using a Quantchrome Autosorb Automated Gas Sorption System. Before each experiment, the samples were evacuated at 573 K for 24 h. The number of available Pt active sites in the Pt/SiO₂–Al₂O₃ catalyst was measured with same equipment by the irreversible H₂ adsorption at 303 K. The catalyst was reduced *in situ* at 723 K for 2 h with H₂ flow before the chemisorption measurement.

2.3. Catalytic activity

The hydrodeoxygenation reaction was carried out in a stainless steel tubular flow reactor heated by a Lindberg (type 54032) furnace. In order to ensure a uniform temperature profile along the catalyst bed, an aluminum filler was inserted in the void between the heating tube of the furnace and tubular reactor. The temperature difference between the middle and top (or end) of the tubular reactor was less than 15 K. Before the reaction, the Pt/SiO₂–Al₂O₃ (the particle size distribution about 100 mesh) was reduced in the reactor with hydrogen flowing from the bottom at about 200 mL min⁻¹. For each activity test, 3.3 g Pt/SiO₂–Al₂O₃ catalyst was used. The temperature regime used for reduction of Pt/SiO₂–Al₂O₃ catalyst was: room temperature to 723 K at 50 K h⁻¹, then hold at 723 K for 2 h. After cooling down the temperature to 493 K and slowly increasing the pressure to 2.93 MPa, the liquid feed (5 wt.% sorbitol aqueous solution) was cofed with the hydrogen (45 mL min⁻¹) to the catalyst from reactor bottom with the help of a JASCO PU980 HPLC pump. A gas–liquid separator was employed after the reactor tube. The gaseous products from the reactor flow through a back pressure regulator, used to maintain the pressure of the reaction system. The gaseous products were further analyzed by two online gas chromatographs (HP 5890 series II). CO₂ in the gaseous product were analyzed by a Thermal Conductivity Detector (TCD). Alltech HAYESEB DB 100/120 packed column (Part no. 2836PC) was used with the oven temperature held constant at 348 K. The TCD and the injection port were held at 433 K and 393 K respectively. The column flow rate was 41 mL min⁻¹ with helium carrier gas. Alkanes in the gaseous product were analyzed on a flame ion detector (FID) with Alltech AT-Q capillary column (Part no. 13950). Helium was used as the carrier gas with the column flow rate of 1 mL min⁻¹. Both the injection port and the detector were held at 473 K. Following GC oven temperature regime was used: hold at 313 K for 6 min, ramp to 453 K at 5 K min⁻¹ and hold at 453 K for 25 min. Liquid product accumulated in the gas–liquid separator was drained then. Liquid product was drained periodically and analyzed by GC–MS and HPLC. The GC–MS is Shimadzu GC-2010 with an Rtx-VMS capillary column. Helium was used as the carrier gas with the column flow rate of 1.57 mL min⁻¹.

Both the injection port and the detector were held at 513 K. For each analysis, 1 μ L liquid sample was injected. The column was held at 308 K for 5 min, ramped to 323 K at 5 K min⁻¹, then to 513 K at 20 K min⁻¹ and kept at 513 K for 7.5 min. A Shimadzu HPLC with UV–Vis (SPD-20AV) and RID (RID-10A) detectors was also used to analysis the liquid products. One microliter liquid sample was injected for each sample. The separation of the products was realized by a BIO-RAD Aminex HPX-87H column (Catalog no. 125-0140) maintained at 303 K with 0.005 M H₂SO₄ as mobile phase flowing at a rate of 0.6 mL min⁻¹. Finally, a total organic carbon (TOC) analyzer (Shimadzu TOC-5000A) was used to check the carbon balance. No major catalyst deactivation was observed during the reactions performed in this study. We tested every reaction in a continuous run of 24 h and did not observe catalyst deactivation. The data were collected after at least 6-h time on stream, and multiple points were collected for each reaction condition.

3. Results

3.1. Characterization of the Pt/SiO₂–Al₂O₃ catalyst

The XRD pattern of the 4 wt.% Pt/SiO₂–Al₂O₃ (omitted here) has only a wide peak at 2 θ range from 15° to 30°, no peak of Pt or its oxide can be observed, which means that the Pt species is well dispersed on the support (less than 5 nm). The catalysts had a hydrogen uptake of 74.25 μ mol \cdot H₂ \cdot g_{catalyst}⁻¹ which corresponds to a H to Pt ratio of 0.724 (*i.e.* 72.4% dispersion). This further affirmed that the Pt was highly dispersed. The specific BET surface area of the Pt/SiO₂–Al₂O₃ catalysts was 430 m² g⁻¹.

3.2. Catalytic activity

3.2.1. Catalytic performance of 4 wt.% Pt/SiO₂–Al₂O₃ with sorbitol

We first investigated the APHDO of a 5 wt.% sorbitol aqueous solution at 518 K, 2.93 MPa at weight hour space velocities (WHSV) from 0.73 h⁻¹ to 11.64 h⁻¹. As shown in Tables 1–4 and Figs. 1–3, a wide variety of products are formed in this reaction. The gas product was mainly composed of CO₂, C1–C6 straight chain alkanes, unreacted H₂ and trace amount of furans (furan, 2-methylfuran, 2,5-dimethylfuran) at high space velocities. No CO peak was observed in the chromatogram which means that the CO concentration is very low. The liquid phase product includes alcohol, diol, polyols, ketones, cyclic ether, isosorbide and unconverted sorbitol. We have been able to identify over 60% of the carbon products that are in the liquid phase and between 70% and 100% of the total carbon products in this study. We are unable to identify all of the carbon because of the following two reasons: (1) some of the products are present as minor components with concentrations below detection limits. (2) some non-volatile oligomers may be formed during the reaction. These oligomers are not detected by our current GC–MS and HPLC. Future work in analytical chemistry will help in identifying more of the carbon in the liquid phase.

As shown in Table 1, the space velocity strongly influences the amount of carbon presenting in the liquid and gaseous phase products. Fig. 1 shows the conversion of sorbitol and carbon distribution in the gas and liquid phase as a function of space velocity. The sorbitol conversion increases almost linearly from 8.1% to 100% as the space velocity decreases from 11.64 h⁻¹ to 2.91 h⁻¹. At space velocities higher than 3 h⁻¹, over 70% of the carbon is still in the liquid phase. As the space velocity decreases further, more and more liquid products are converted into gas phase products.

Fig. 2 shows the distribution of products in the gas and liquid phases. At high space velocities, over 80% of the gas is CO₂. The CO₂ is most likely produced from the decarbonylation of aldehydic species. Decarbonylation produces CO which is converted into CO₂

Table 1
Conversion to gas and liquid products as a function of WHSV for sorbitol conversion over 4 wt.% Pt/SiO₂-Al₂O₃ catalyst. (Reaction conditions: 5 wt.% sorbitol aqueous phase solution, 518 K, 2.93 MPa and flow rate of H₂ about 45 mL min⁻¹.)

WHSV of liquid (h ⁻¹) ^a	CH ₂ at inlet (mol L ⁻¹) ^b	C _{sorbitol} at inlet (mmol L ⁻¹) ^c	Carbon in gas phase detected by GC (%)	Carbon in liquid phase detected by TOC analysis (%)	Carbon balance (%)	% of liquid products and reactants identified by GC-MS and HPLC (%)
0.73	0.668	3.99	82.1	18.2	100.3	74.2
1.45	0.660	7.46	61.0	36.1	97.1	90.3
2.91	0.643	14.3	23.9	75.1	99.0	67.1
5.82	0.617	24.7	9.2	92.5	101.7	58.0
11.64	0.562	47.2	1.8	100.0	101.8	104.7

^a Weight hourly space velocity (WHSV in units of h⁻¹) = (mass flow rate of feed solution in the unit of h⁻¹)/(the mass of catalyst).

^b CH₂ at inlet (mol L⁻¹) = (Mol of H₂ fed into the reactor)/(sum of the volume of gas and liquid at the reaction condition). Assumes the liquid volume does not change with temperature.

^c C_{sorbitol} at inlet (mmol L⁻¹) = (Mol of sorbitol fed into the reactor) × 1000/(sum of the volume of gas and liquid at the reaction condition). Assumes the liquid volume does not change with temperature.

Table 2
Selectivity of C6 compounds in the liquid product as the function of WHSV. Reaction conditions: 5 wt.% sorbitol aqueous phase solution, 518 K, 2.93 MPa and flowrate of H₂ about 45 mL min⁻¹ with inlet concentrations listed in Table 1.

WHSV (h ⁻¹)	Yield of C6 (%) ^a		Sorbitol left in the solution (%)	Selectivity (%)							
	Gas phase	Liquid phase		Hexanol ^b	Hexanone ^c	2-Methyl-tetra-hydro-pyran	2,5-Dimethyl-tetra-hydro-furan	1,2-Hexanediol	Tetra-hydro-pyran-2-methanol	1,2,6-Hexanetriol	Isosorbide
0.73	17.6	0.5	0	29.8	0	70.2	0	0	0	0	0
1.45	8.9	7.9	0	57.2	18.5	5.6	10.4	0	3.0	5.3	0
2.91	1.73	20.1	0	9.0	25.8	2.5	10.2	15.6	10.0	26.1	0.8
5.82	0.59	16.7	19.7	2.0	8.7	0.44	0	10.3	2.5	15.4	60.5
11.64	0.027	13.9	81.0	0	0	0	0	0	0	0	100

^a Yield of C6 (%) = (the sum of carbon in C6 compound in gas or liquid products)/(the carbon in the feed solution) × 100%.

^b The hexanol includes 1-hexanol, 2-hexanol, and 3-hexanol. The amount of 1-hexanol and 2-hexanol are comparable. Both of them are much higher than that of 3-hexanol.

^c The hexanone include 2-hexanone and 3-hexanone. The concentration of 2-hexanone and 3-hexanone are very similar.

Table 3
Selectivity of C1–C3 compounds in the liquid product as the function of WHSV. Reaction conditions: 5 wt.% sorbitol aqueous phase solution, 518 K, 2.93 MPa and flowrate of H₂ about 45 mL min⁻¹ with inlet concentrations listed in Table 1.

WHSV (h ⁻¹)	Yield of C1–C3 (%) ^a		Selectivity (%)							
	Gas phase	Liquid phase	Methanol	Ethanol	Propanol ^b	Acetone	Ethylene glycol	1,2-Propanediol	2-Hydroxy-acetone	Glycerol
0.73	45.3	11.2	13.9	32.3	53.7	0	0	0	0	0
1.45	39.2	10.7	10.5	35.8	51.5	2.2	0	0	0	0
2.91	18.5	11.5	3.4	14.2	16.2	3.3	3.7	56.4	2.6	0
5.82	8.1	9.2	3.2	10.1	6.8	0	5.2	47.6	11.6	15.4
11.64	1.7	4.7	1.6	4.8	0	0	16.4	38.2	13.5	25.4

^a Yield of C1–C3 (%) = (the sum of carbon in C1–C3 compound in gas or liquid products)/(the carbon in the feed solution) × 100%.

^b The propanol include 1-propanol and 2-propanol. Then concentration of 2-propanol is more than five times of that of 1-propanol.

and H₂ by the water–gas shift reaction. It has previously been shown that the water–gas shift reaction is in near equilibrium under APHDO conditions [25]. As the space velocity decreases, the gas phase C2–C6 selectivity increases, while the C1 product selectivity (which is primarily CO₂) decreases. The liquid phase carbon selectivities are shown in Fig. 2b. The amount of C6 products in the liquid phase increases with space velocity. The C6 product yield reaches the maximum at space velocity of 2.91 h⁻¹ then decreases as the space velocity decreases. The C6 products are shown in Table 2. The C6 products that are formed include isosorbide, 1,2,6-hexanetriol, tetrahydropyran-2-methanol, 1,2-hexanediol, 2,5-dimethyltetrahydrofuran, 2-methyl-tetrahydropyran, hexanone, and hexanol. We observed 100% isosorbide selectivity at a space velocity of 11.64 h⁻¹. The isosorbide selectivity decreases from 100% to 60.5% as the space velocity decreases from 11.64 h⁻¹ to 5.82 h⁻¹. As the WHSV decreases further to 2.91 h⁻¹, the C6 selectivity of isosorbide then decreases to 0.8%. 1,2,6-Hexanetriol is observed as a major product. The 1,2,6-hexanetriol C6 liquid selectivity increases from 15.4% to 26.1% as the WHSV decreases

from 5.82 h⁻¹ to 2.91 h⁻¹. Then the selectivity of 1,2,6-hexanetriol decreases as the WHSV decreases below 2.91 h⁻¹. At WHSV of 2.91 h⁻¹ and below, the major C6 liquid products include a combination of hexanediols, hexanols and some saturated cyclic ether compounds (2-methyl-tetrahydropyran, 2,5-dimethyltetrahydrofuran, tetrahydropyran-2-methanol).

As shown in Fig. 2b and Table 2, at a space velocity of 11.64 h⁻¹, over 95% of the liquid products are C6 compounds. The other 5% of the products are primarily C3 compounds which are primarily 1,2-propanediol (38% C1–3 selectivity), glycerol (25.4% C1–C3 selectivity), and hydroxyacetone (13.5% C1–C3 selectivity) as shown in Table 3. These products are produced primarily from retro-aldol condensation. As the space velocity decreased further, the amount of liquid phase C1–C3 products increases. However, the distribution of C1–C3 products (reported in Table 3) is primarily the alcohols. At a higher space velocities, the majority of the products are C2 and C3 polyols including 1,2-propanediol, glycerol, hydroxyacetone, and ethylene glycol. As the WHSV decreases below 2.91 h⁻¹, the selectivity to these products decreases and the C1–C3 products

Table 4

Selectivity of C4–C5 compounds in the liquid product as the function of WHSV. Reaction conditions: 5 wt.% sorbitol aqueous phase solution, 518 K, 2.93 MPa and flowrate of H₂ about 45 mL min⁻¹ with inlet concentrations listed in Table 1.

WHSV (h ⁻¹)	Yield to C4–C5 (%) ^a		Selectivity (%)								
	Gas phase	Liquid phase	Butanol ^b	Pentanol ^c	Butanone	2-Pentanone	Tetrahydro-pyran	2-Methyl-tetrahydro-furan	Butanediol ^d	1,2-Pentanediol	Tetra-hydro-furfural alcohol
0.73	19.2	1.7	37.8	26.2	0	0	36.0	0	0	0	0
1.45	12.9	14.0	14.9	32.1	30.8	0	5.9	8.9	2.4	2.9	2.1
2.91	3.7	19.0	3.6	7.3	32.3	3.9	2.4	8.7	20.5	18.4	2.9
5.82	0.54	8.8	0	4.1	0	4.2	2.7	0	36.2	46.9	5.9
11.64	0.075	0.4	0	0	0	0	0	0	74.4	25.6	0

^a Yield of C4–C5 (%) = (the sum of carbon in C4–C5 compound in gas or liquid products)/(the carbon in the feed solution) × 100%.

^b The butanol include 1-butanol and 2-butanol. The concentration of 1-butanol is much higher than that of 2-butanol, indicating that most of butanol is 1-butanol.

^c The pentanol include 1-pentanol and 2-pentanol. The amount of 1-pentanol is more than eight times of that for 2-pentanol.

^d The butanediol include 1,2-butanediol and 2,3-butanediol. More than 60% of butanediol detected are 1,2-butanediol.

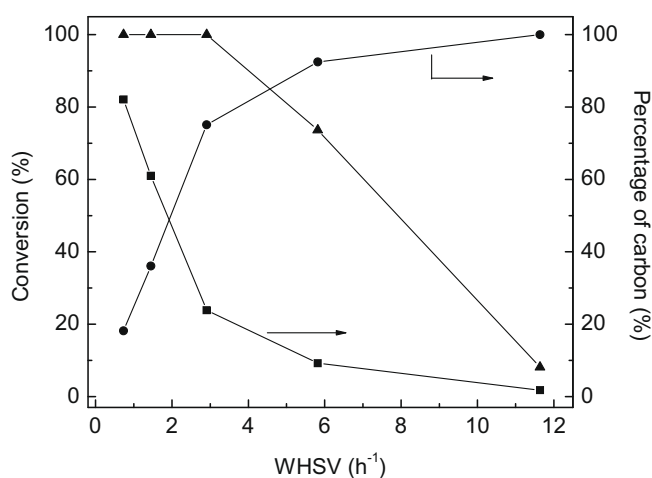


Fig. 1. Sorbitol conversion (▲), gas phase carbon (■) and liquid phase carbon (●) as a function of weight hour space velocity (WHSV). Reaction conditions: 5 wt.% sorbitol aqueous phase solution, 518 K, 2.93 MPa and flowrate of H₂ about 45 mL min⁻¹ with inlet concentrations listed in Table 1.

are mainly alcohols including methanol, ethanol and propanol. The yield of C1–C3 products increases with decreasing WHSV. This data suggest that the C2 and C3 polyols are produced from the sorbitol by retro-aldol condensation.

A wide variety of C4–C5 oxygenates are formed as shown in Table 4. The yield of C4–C5 oxygenates increases from 0.4% to 38.7% as the space velocity decreases from 11.64 h⁻¹ to 1.45 h⁻¹. The yield of C4–C5 oxygenates decreases as the space velocity decreases from 1.45 h⁻¹ to 0.73 h⁻¹. At high space velocities (above 5.82 h⁻¹), the C4–C5 products are 1,2-pentanediol, 1,2-butanediol and 2,3-butanediol. Importantly, no C4–C5 oxygenates were identified that have more than two oxygenates. This indicated that C4 and C5 molecules are only formed after a large majority of the oxygen is removed from the biomass feedstock. At space velocities lower than 2.91 h⁻¹, the major C4 and C5 products are alcohols (1-butanol, 2-butanol, 1-pentanol, 2-pentanol) and ketones (butanone, 2-pentanone). A small amount of tetrahydropyran, 2-methyl-tetrahydrofuran, tetrahydrofurfural alcohol are also formed in this process.

Fig. 3 shows the overall selectivity of C1–C6 carbon distribution which was calculated by taking into consideration of carbon exists in both the liquid and the gas phase. At high space velocity, the majority of the carbon is present as C6 products. The C6 product selectivity decreases from 94% to 36% as the space velocity

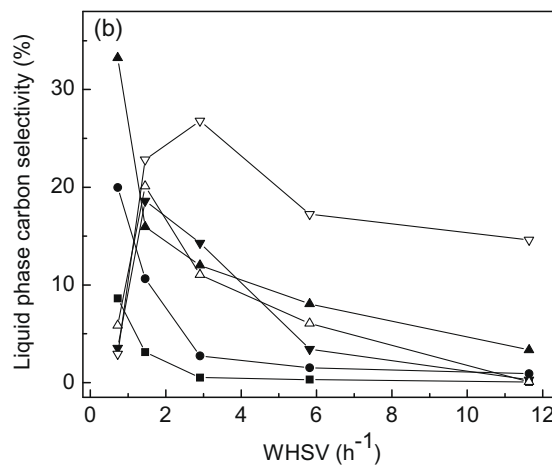
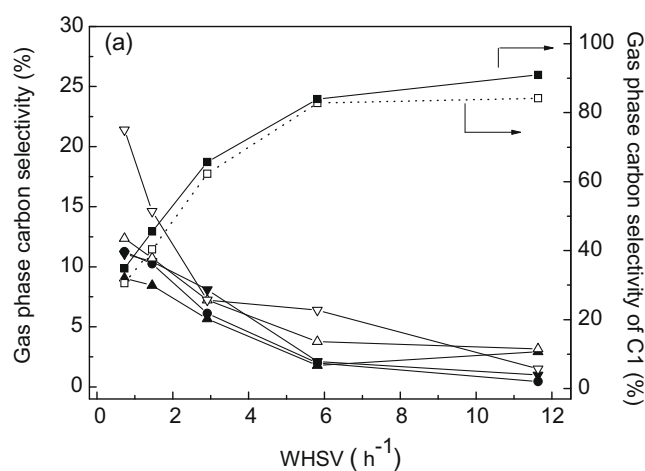


Fig. 2. Gas phase (a) and liquid phase (b) carbon selectivity of C1 (■), C2 (●), C3 (▲), C4 (▼), C5 (△), C6 (▽) and CO₂ (□) as a function of WHSV. Reaction conditions: 5 wt.% sorbitol aqueous phase solution, 518 K, 2.93 MPa and flowrate of H₂ about 45 mL min⁻¹ with inlet concentrations listed in Table 1.

decreases from 11.64 h⁻¹ to 5.82 h⁻¹. The C6 selectivity then decreases from 36% to 22% as the space velocity decreases from 5.82 h⁻¹ to 2.91 h⁻¹. As the space velocity decreases further, the C6 product selectivity does not change significantly. This indicates that the majority of the C–C bond cleavage for the C6 products occurs very early on. The overall product selectivity of C1 compounds increases as the space velocity decreases from 11.64 h⁻¹ to 0.73 h⁻¹.

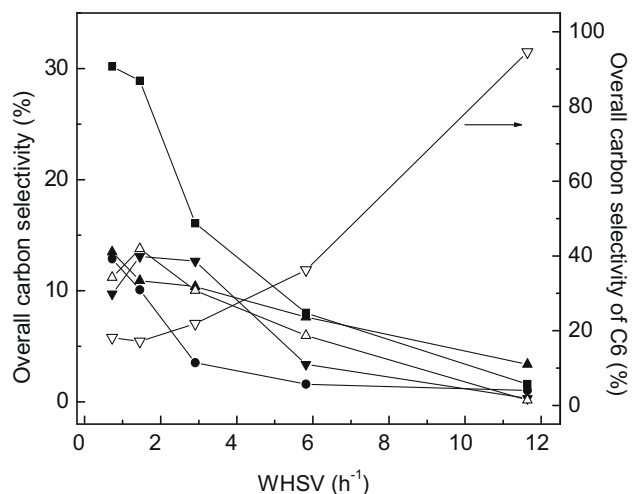


Fig. 3. Overall carbon selectivity of C1 (■), C2 (●), C3 (▲), C4 (▼), C5 (△), C6 (▽) as a function of WHSV. Reaction conditions: 5 wt.% sorbitol aqueous phase solution, 518 K, 2.93 MPa and flowrate of H₂ about 45 mL min⁻¹ with inlet concentrations listed in Table 1.

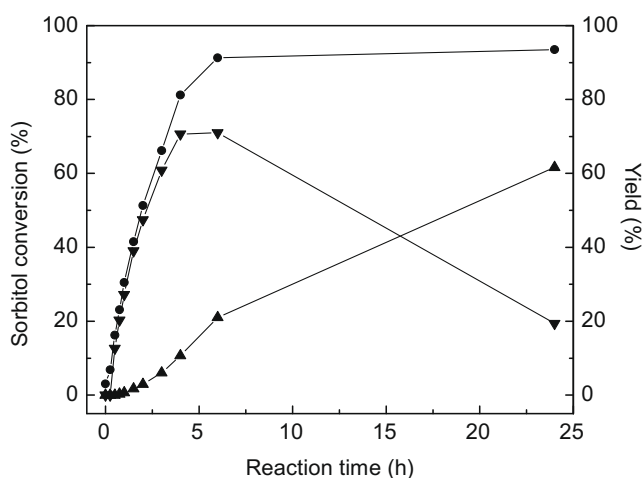


Fig. 4. Conversion of sorbitol (●), the yield of 1,4-sorbitan (▼) and isosorbide (▲) over pure SiO₂-Al₂O₃ support as the function of reaction time. Reaction condition: 90 mL 5 wt.% sorbitol aqueous solution, 0.9 g SiO₂-Al₂O₃ catalyst, 518 K, 2.93 MPa.

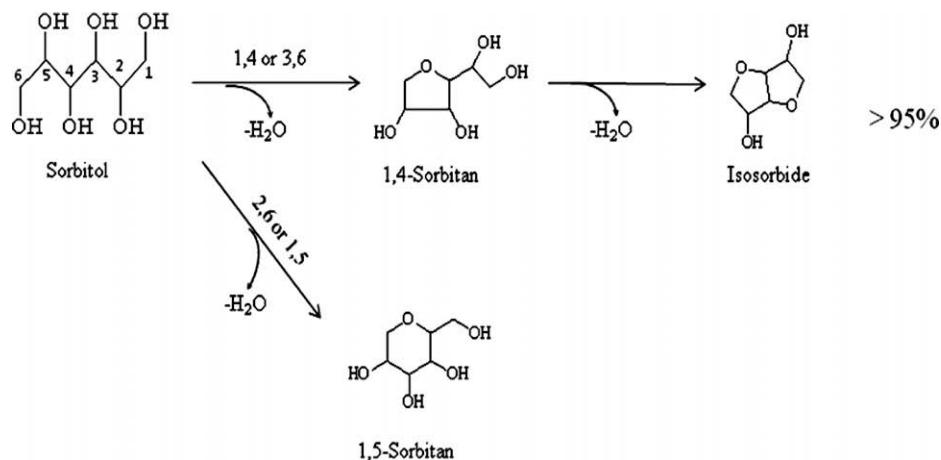


Fig. 5. Major reaction pathways for dehydration of 5 wt.% sorbitol aqueous solution over SiO₂-Al₂O₃ catalyst at 518 K.

3.2.2. Dehydration of sorbitol over pure SiO₂-Al₂O₃ support

We also investigated the dehydration of 5 wt.% sorbitol solution over the SiO₂-Al₂O₃ support at the same temperature under inert atmosphere (Helium) as shown in Fig. 4. The work was done with a batch reactor. Only C6 compounds (1,4-sorbitan, isosorbide and trace amount of 1,5-sorbitan) were detected, which means that no C–C bond cleavage took place during the dehydration step. In other words, the metal catalytic sites are necessary for C–C bond cleavage. Fig. 5 illustrates the pathways for sorbitol dehydration. We can see that the dehydration of sorbitol to isosorbide is a two-step reaction: in the first step, the sorbitol is intermolecularly dehydrated to 1,4-sorbitan. Subsequently, the 1,4-sorbitan is further dehydrated to isosorbide.

3.2.3. Hydrodeoxygenation of model compounds over Pt/SiO₂-Al₂O₃ catalyst

We studied the APHDO of a series of model compounds including isosorbide, 1,2,6-hexanetriol, 1,2-hexanediol, 2,3-butanediol, 1-butanol and 2-butanol. The concentrations of all model compounds were fixed at 5 wt.% with a reaction temperature and pressure of 518 K and 2.93 MPa.

3.2.3.1. Hydrodeoxygenation of isosorbide and 1,2,6-hexanetriol. To further understand the conversion of sorbitol after dehydration, we also investigated the APHDO of isosorbide and 1,2,6-hexanetriol, and the results are shown in Tables 5 and 6.

From Table 5, we observed that isosorbide has a significantly higher gas phase alkane selectivity and hexane selectivity compared to sorbitol or hexanetriol. For example, at a WHSV = 0.73 h⁻¹, a 90% alkane selectivity and 65% hexane selectivity can be obtained for isosorbide. In comparison, under the same reaction conditions with sorbitol as the feed, the alkane and hexane selectivity are about 70% and 30% respectively. In contrast to sorbitol, the gas phase alkane selectivity for isosorbide is not a strong function of conversion. With the isosorbide as feed stock, when WHSV increased from 0.73 h⁻¹ to 2.91 h⁻¹, the carbon selectivity to CO₂ did not change, but the selectivity to hexane even increased a little bit from 64.9% to 80.5%, which can be explained by the retraining of the cyclic opening reaction over the acid sites by decreasing the contacting time between isosorbide and catalyst. From Table 6, we can see that all the intermediates identified from the liquid product of APHDO of isosorbide are similar to the products we detected with sorbitol as feed stock, which indicates that isosorbide is a key intermediate for the APHDO of sorbitol over Pt/SiO₂-Al₂O₃.

Table 5

Activity and selectivity of 4 wt.% Pt/SiO₂-Al₂O₃ catalyst for the aqueous-phase hydrodeoxygenation (APHDO) of isosorbide, 1,2,6-hexanetriol and sorbitol. Reaction conditions: 5 wt.% aqueous phase solution, 518 K, 2.93 MPa and flow rate of H₂ about 45 mL min⁻¹.

Feedstock	WHSV (h ⁻¹)	Carbon conversion to gas (%) from GC ^a	Alkane selectivity (%) ^b	CO ₂ selectivity (%)	Specific alkane selectivity (%) ^c					
					C1	C2	C3	C4	C5	C6
Isosorbide	0.73	68.9	89.1	10.9	1.2	3.4	4.2	7.0	19.3	64.9
Isosorbide	2.91	12.5	89.2	10.8	0.7	2.6	3.0	4.2	9.0	80.5
1,2,6-hexanetriol	0.73	66.2	70.2	29.8	0.20	0.04	3.02	38.2	44.2	14.3
1,2,6-hexanetriol	1.45	44.8	66.3	33.7	0.12	0.03	3.08	36.8	46.0	14.1
1,2,6-hexanetriol	2.91	16.7	51.4	48.6	0.18	0.04	3.61	40.4	40.1	15.8
Sorbitol	0.73	82.1	68.8	31.2	5.5	14.9	12.6	16.9	19.5	30.4
Sorbitol	1.45	61.0	59.7	40.3	8.7	17.2	14.1	17.5	18.0	24.5
Sorbitol	2.91	23.9	37.7	62.3	9.0	16.2	15.0	21.4	19.2	19.1

^a Carbon conversion to gas (%) from GC = (sum of the carbon detected by GC)/(carbon in the feed solution) × 100%.

^b Alkane selectivity (%) = (sum of carbon in alkanes detected by GC)/(sum of carbon detected in gas phase) × 100%.

^c Specific alkane selectivity (%) = (carbon in specific alkanes)/(sum of carbon in alkanes detected by GC) × 100%.

Table 6

Liquid product selectivity (%)^a for the APHDO of isosorbide and 1,2,6-hexanetriol over 4 wt.% Pt/SiO₂-Al₂O₃ catalyst at different WHSV. Reaction conditions: 5 wt.% aqueous phase solution, 518 K, 2.93 MPa and flow rate of H₂ about 45 mL min⁻¹.

Carbon number	Component	Isosorbide		1,2,6-Hexanetriol		
		0.73 h ⁻¹	2.91 h ⁻¹	0.73 h ⁻¹	1.45 h ⁻¹	2.91 h ⁻¹
C1	Methanol	0	0.1	0	0	0
C2	Ethanol	4.3	0.5	0	0	0
C3	Propanol ^b	17.6	1.0	0	0	0
	1,2-Propanediol	0	0.9	0	0	0
C4	Butanol ^c	6.8	0.5	4.9	3.8	3.1
	Tetrahydrofuran	0.7	0.1	0	0	0
	2,3-Butanediol	0	1.2	0	0	0
C5	Pentanol ^d	7.8	0.8	39.1	38.8	32.7
	Pentanal	0	0	0	0	0.8
	2-Pentanone	0	0.6	0	0	0
	Tetrahydropyran	2.0	0.2	31.6	12.4	6.5
	2-Methyl-tetrahydrofuran	2.1	1.3	0	0	0
	Tetra-hydrofurfural alcohol	4.9	1.5	0	0	0
	1,2-Pentanediol	0	0	0	0	8.8
1-Hydroxy-2-pentanone	30.3	8.5	0	0	0	
C6	Hexanol ^e	20.0	4.9	9.1	15.7	17.6
	Hexanone ^f	0	5.2	0	0	0.7
	2-Methyl-tetrahydropyran	2.5	0	5.9	4.5	3.3
	2,5-Dimethyltetrahydrofuran	2.3	0.6	0	0	0
	Oxepane	0	0	4.6	3.4	1.7
	Tetrahydropyran-2-methanol	1.5	0.4	4.9	20.4	23.9
	1,2-Hexanediol	0	4.1	0	0	0
	1,2,6-Hexanetriol	1.5	0.6	0	0	0
Isosorbide	0	67.1	0	0	0	

^a The value in the table is the carbon selectivity (%) of specific compound in the liquid phase.

^b The propanol includes 1-propanol and 2-propanol. The concentration of 1-propanol is more than 40 times of 2-propanol.

^c The butanol includes 1-butanol and 2-butanol. For 1,2,6-hexanediol, the butanol detected is totally 1-butanol. While for isosorbide, the butanol is 2-butanol.

^d The pentanol includes 1-pentanol and 2-pentanol. The amount of 1-pentanol is more than 30 times of 2-pentanol.

^e The hexanol includes 1-hexanol, 2-hexanol and 3-hexanol. The concentration of 1-hexanol is more than twice of 2-hexanol and 3-hexanol.

^f The hexanone includes 2-hexanone and 3-hexanone. For 1,2,6-hexanetriol, only 2-hexanone was detected. For isosorbide, the concentration of 3-hexanone is more than twice of 2-hexanone.

As shown in Table 5, when 1,2,6-hexanetriol was the feedstock, propane, butane, pentane, hexane and CO₂ are the main products. The selectivity to methane and ethane are very low (less than 1%). This result indicates the C–C bond cleavage for oxygenates mainly occurs at the C with C–O bond.

The alkane selectivity for 1,2,6-hexanetriol is only slightly higher than sorbitol, the hexane selectivity is also lower for hexanetriol than sorbitol. However, the butane and pentane selectivity is much higher than either sorbitol or isosorbide. The gas phase carbon conversion decreases with increasing space velocity. The CO₂ selectivity increases slightly with increasing space velocity and the alkane selectivity does not change significantly with space velocity. After the analysis of liquid products (illustrated in Table 6), some cyclic ether species (such as tetrahydropyran, tetrahydrofurfural alcohol,

tetrahydropyran-2-methanol, 2-methyl-tetrahydropyran, oxepane) were detected. We also noticed from Table 6 that the selectivities of 6-ring cyclic ethers (tetrahydropyran, 2-methyl-tetrahydropyran, tetrahydropyran-2-methanol) are higher than of 7-ring cyclic ether (oxepane). The pathway for the APHDO of 1,2,6-hexanetriol is shown in Fig. 6.

3.2.3.2. Hydrodeoxygenation of 1,2-hexanediol and 2,3-butanediol. Subsequently, we also investigated the APHDO of diols including 1,2-hexanediol and 2,3-butanediol. These compounds were selected because their hydroxyl groups are in different positions: The 1,2-hexanediol represents the diols with OH locates respectively at the edge and in the middle of molecule. The 2,3-

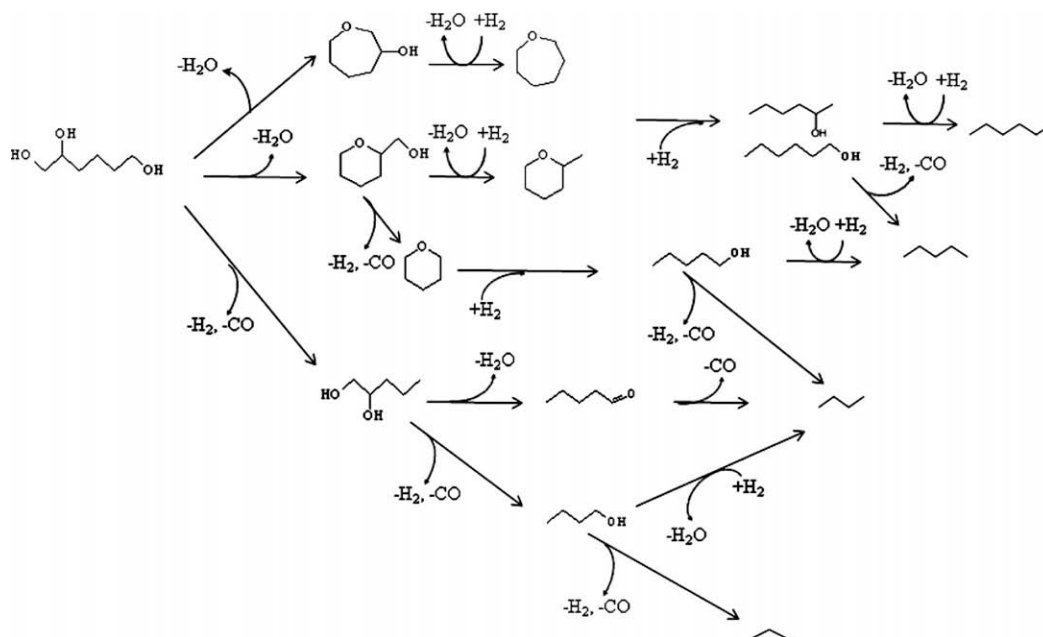


Fig. 6. Major reaction pathways for hydrodeoxygenation of 1,2,6-hexanetriol at 518 K.

butanediol stands for the diols with both OH groups in the middle of molecule.

As shown in Table 7, 1,2-hexanediol produced propane, butane, hexane and CO₂. The selectivity of propane, butane and CO₂ increased with the space velocity, which is due to the preferable C–C bond cleavage at higher space velocity. It seems that the effect of space velocity on the C–C cleavage of 1,2-hexanediol is more significant than 1,2,6-hexanetriol even though the latter has more OH groups at the end of the molecules, this phenomena can be rationalized by the generation of cyclic ether (tetra-hydropyran-2-methanol and 2-oxepanol). As we know, the formation of

relative stable cyclic ether can (partially) eliminate the number of OH at the edge of 1,2,6-hexanetriol. As a direct result, the C–C bond cleavage by the decarbonylation of aldehyde was inhibited.

From the liquid phase analysis (cf. Table 8), 1-pentanol, 1-hexanol, 2-hexanol, 2-hexanone were identified as intermediates. Reaction routes were shown in Fig. 7. We can see that the APHDO of 1,2-hexanediol produces 1-pentanol. This is then converted into butane by dehydrogenation and decarbonylation. The main gas phase products for 2,3-butanediol are butane, propane and CO₂. With the increasing of space velocity, the selectivity does not change. After analysis the liquid phase products, 2-butanol,

Table 7
Activity and selectivity for the APHDO of 1,2-hexanediol and 2,3-butanediol over 4 wt.% Pt/SiO₂-Al₂O₃ catalyst. Reaction conditions: 5 wt.% 1,2-hexanediol and 2,3-butanediol aqueous phase solution, 518 K, 2.93 MPa and flow rate of H₂ about 45 mL min⁻¹.

Compound	WHSV (h ⁻¹)	Carbon conversion to gas (%) from GC	Alkane selectivity (%)	CO ₂ selectivity (%)	Specific alkane selectivity (%)					
					C1	C2	C3	C4	C5	C6
1,2-Hexanediol	0.73	76.0	85.6	14.4	0.1	0.0	0.0	9.6	48.4	41.6
1,2-Hexanediol	1.45	40.0	77.0	23.0	0.1	0.0	0.0	20.9	53.0	26.0
2,3-Butanediol	0.73	100.0	96.5	3.5	0.0	0.1	9.6	90.2	0	0
2,3-Butanediol	1.45	69.1	95.5	4.5	0.0	0.2	12.2	87.6	0	0

Table 8
Liquid product selectivity (%)^a for the APHDO of 1,2-hexanediol and 2,3-butanediol over 4 wt.% Pt/SiO₂-Al₂O₃ catalyst at different WHSV. Reaction conditions: 5 wt.% aqueous phase solution, 518 K, 2.93 MPa and flow rate of H₂ about 45 mL min⁻¹.

Carbon number	Component	1,2-Hexanediol		2,3-Butanediol	
		0.73 h ⁻¹	1.45 h ⁻¹	0.73 h ⁻¹	1.45 h ⁻¹
C3	2-Propanol	0	0	0	0.7
	Acetone	0	0	0	0.2
C4	2-Butanol	0	0	26.4	18.7
	2-Butanone	0	0	73.6	79.2
	2,3-Butanediol	0	0	0	1.1
C5	1-Pentanol	98.4	65.1	0	0
C6	1-Hexanol	1.6	0.7	0	0
	2-Hexanol	0	34.1	0	0
	2-Hexanone	0	0.06	0	0
	1,2-Hexanediol	0	0.03	0	0

^a The value in the table is the carbon selectivity (%) of specific compound in the liquid phase.

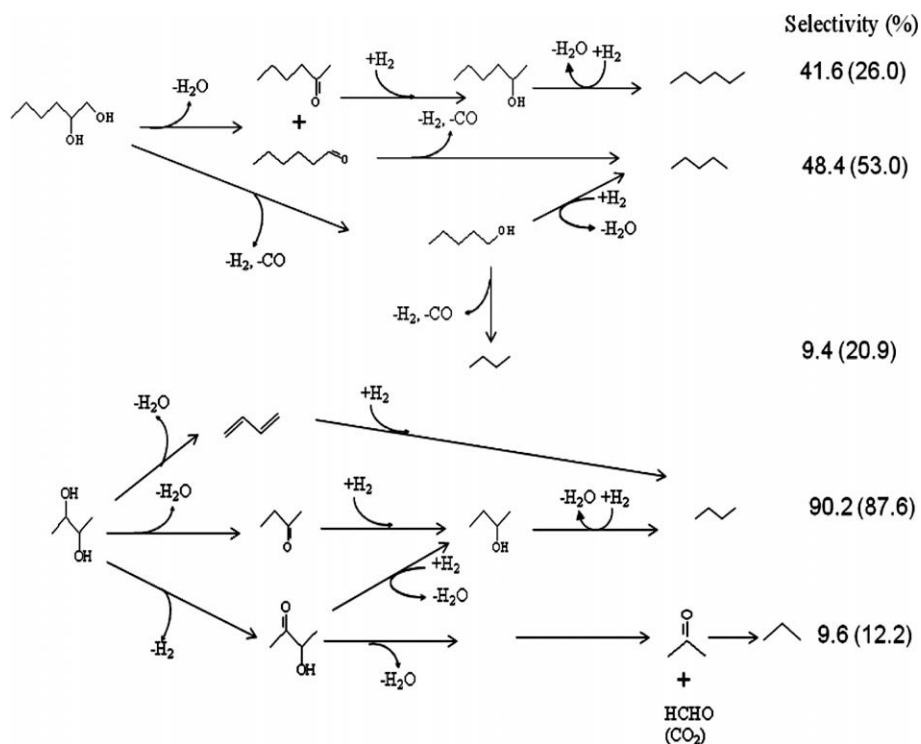


Fig. 7. Major reaction pathways for hydrodeoxygenation of 1,2-hexanediol and 2,3-butanediol over the 4 wt.% Pt/SiO₂-Al₂O₃ catalyst at 518 K.

butanone, isopropanol and acetone were identified as intermediates. The reaction pathways as shown in Fig. 7 were drawn.

3.2.3.3. *Hydrodeoxygenation of 1-butanol and 2-butanol.* Table 9 lists the result from the analysis of gas phase products from the APHDO of 5 wt.% 1-butanol and 2-butanol in aqueous solutions at 518 K and 2.93 MPa. For 1-butanol, butane, propane and CO₂ were identified as the final products. Higher CO₂ and propane selectivity were observed at higher space velocity, indicating that the C–C

bond cleavage is more preferable under such condition. In contrast, for 2-butanol, butane is the only product (no C–C bond cleavage occurs). The liquid product only contains unreacted 1-butanol or 2-butanol indicating that the intermediates are not stable. 2-butanol is more reactive than 1-butanol. This is because a second carbocation is more stable than primary carbocation.

We propose the reaction pathways for 1-butanol and 2-butanol as shown in Fig. 8. Both 1-butanol and 2-butanol can be dehydrated to butylenes then hydrogenated to butane. The difference

Table 9

Activity and selectivity for the APHDO of 1-butanol and 2-butanol over 4 wt.% Pt/SiO₂-Al₂O₃ catalyst. Reaction conditions: reaction conditions: 5 wt.% butanol aqueous phase solution, 518 K, 2.93 MPa and flow rate of H₂ about 45 mL min⁻¹.

Compound	WHSV (h ⁻¹)	Carbon conversion to gas (%) from GC	Alkane selectivity (%)	CO ₂ selectivity (%)	Specific alkane selectivity (%)			
					C1	C2	C3	C4
1-Butanol	0.73	51.7	82.9	17.1	0.0	0.0	57.6	42.4
1-Butanol	1.45	40.6	81.7	18.3	0.0	0.0	69.8	30.1
2-Butanol	0.73	98.9	100	0	0.0	0.0	0.0	100.0
2-Butanol	1.45	96.0	100	0	0.0	0.0	0.0	100.0

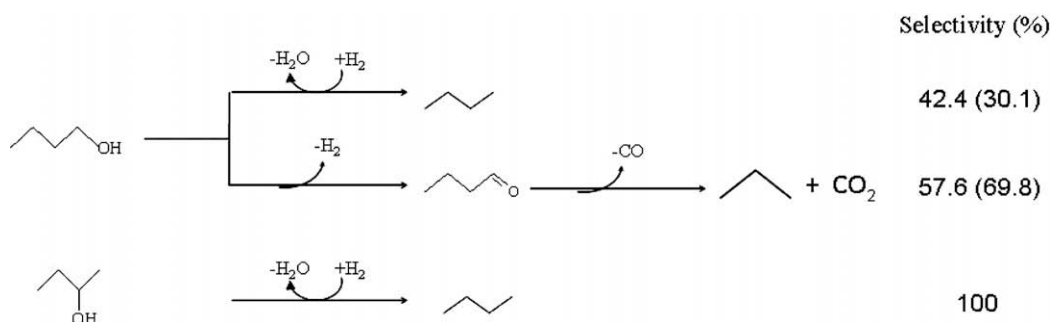


Fig. 8. Major reaction pathways for the hydrodeoxygenation of 1-butanol and 2-butanol over 4 wt.% Pt/SiO₂-Al₂O₃ catalyst at 518 K.

Decarbonylation occurs by C–C bond cleavage of aldehydes on the metal surface forming a CO. The aldehydes are generated by the dehydrogenation of primary alcohol or polyol over metal surfaces. In our reaction, we do not detect large amounts of aldehydes because these species are very reactive and will either undergo hydrogenation or decarbonylation. Dumesic et al. [27] have studied how C–C bonds are broken for ethanol-derived surface species over a Pt surface. These results indicate what may happen in our reaction chemistry for the surface chemistry for decarbonylation of an alcohol or polyol. Ethanol initially adsorbs on the surface most likely as a hydroxyethyl species. The adsorbed hydroxyethyl species then undergoes dehydrogenation reactions to form adsorbed carbonyl species and hydrogen. These adsorbed carbonyl species include acetyl (CH_3CO), ketene (CH_2CO) and ketylenyl (CHCO). The species that has the lowest C–C bond cleavage is the ketylenyl species. They also show that the rate of C–C bond cleavage is significantly lower than the rate of C–O bond cleavage on Pt surfaces. This suggests that C–C bond cleavage by decarbonylation occurs by three major steps: (1) adsorption of the alcohol on the surface; (2) dehydrogenation of the adsorbed species to a carbonyl compounds and (3) C–C bond cleavage.

Retro-aldol condensation reactions occur primarily only for sorbitol on the metal catalytic site. This reaction produces primarily C2 and C3 oxygenates. It has previously been shown that sorbitol can be converted into glycerol, 1,2-propanediol and ethylene glycol over a series of noble metal-based [28–34] catalysts by retro-aldol reactions. These are the same products that we observe for hydrodeoxygenation of sorbitol over $\text{Pt}/\text{SiO}_2\text{-Al}_2\text{O}_3$. A hydroxyl group at the third C atom or a C=C between the second and third carbon atoms is also necessary for this reaction. In our case, the retro-aldol condensation is most likely to happen at the very beginning of the reaction when there are more oxygen atoms on the feed molecule.

A pathway for retro-aldol condensation of sorbitol is shown in Fig. 10. The first step in this pathway is dehydrogenation of sorbitol

which most likely occurs on metal catalytic sites. The ketone can form at either the two or three site of the sorbitol. C–C bond cleavage can then occur at the adjacent carbon atom by retro-aldol condensation. According to literature, this step can happen at acid [35–37], basic [29,34,38,39] or even neutral conditions [29]. The glyceraldehyde and dihydroxyacetone are produced when sorbitol is dehydrogenated at two site. These products can be hydrogenated to glycerol and then further converted to 1,2-propanediol by dehydration/hydrogenation. In contrast, for sorbitol dehydrogenated at three sites, hydroxyl-acetaldehyde and erythrose are generated as the products of retro-aldol condensation. The erythrose can be hydrogenated to threitol or can undergo further retro-aldol condensation to two hydroxyl-acetaldehyde. Hydroxyl-acetaldehyde can be hydrogenated to form glycol. We have been unable to identify the aldehydes that form in the reaction pathway in Fig. 10 probably primarily due to the high concentration of hydrogen in our reactor.

4.3. Carbon–oxygen bond cleavage reactions

Carbon oxygen bond cleavage occurs by dehydration mainly over Brønsted acid catalyst sites. For APHDO of sorbitol, a number of different functionalities are hydroxyl including polyols and alcohols. Dehydration of polyols is done through three different routes: C–O–C bond formation, C=O bond formation and C=C bond formation. If large amounts of oxygen are present on the molecules then C–O–C bonds will be formed as is the case for dehydration of sorbitol and 1,4-sorbitan. This type of dehydration results in the formation of 5- and 6-member rings. For C–O–C bonds to form, there must be hydroxyl groups in the correct positions on the feedstocks.

Dehydration of diols with adjacent hydroxyl groups (e.g. 1,2- or 2,3- polyols) results in a C=O group and water as shown in Fig. 7. This is in agreement with dehydration experiments performed by Olah and co-workers on dehydration of diols [40]. From the carbon

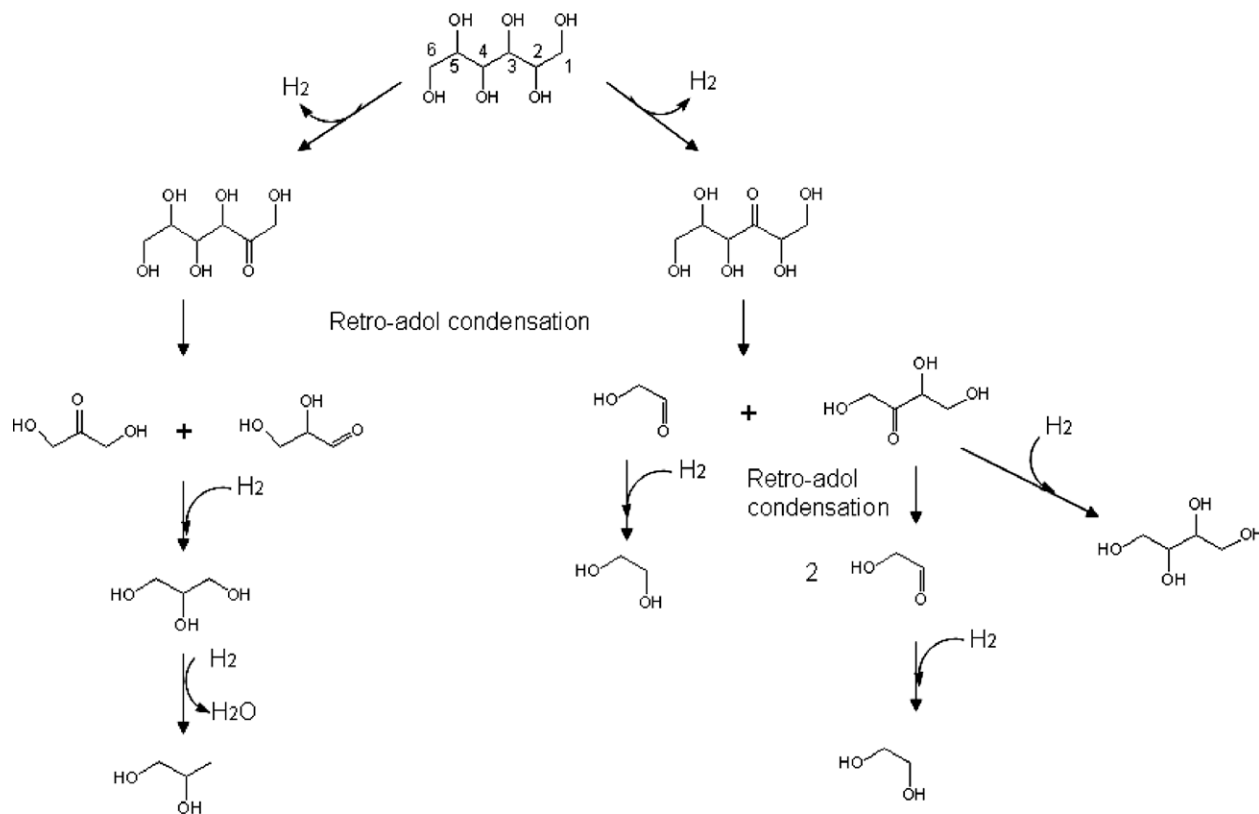


Fig. 10. Reaction pathways for dehydrogenation and retro-aldol condensation of sorbitol.

conversion to gas phase of 1,2-hexanediol and 2,3-butanediol (see Table 7) at the same WHSV, the APHDO of 2,3-butanediol is relatively faster than the APHDO of 1,2-hexanediol. Moreover, as we noticed in the APHDO of sorbitol, the concentration of 1,2-butanediol in the liquid product is also higher than that of 2,3-butanediol.

Dehydration of alcohols results in the formation of C=C bonds and water. The rate of dehydration is a function of the location of the alcohol on the molecules. As shown in Table 9, the rate of dehydration of 2-butanol is significantly higher than the rate of dehydration of 1-butanol. The rate of dehydration of alcohols is known to decrease for tertiary alcohols > secondary alcohols > primary alcohols [41–43]. Dehydration occurs through formation of carbocations with the stability of the carbocation decreasing as tertiary carbocation > secondary carbocation > primary carbocation. It should be noted that for APHDO of sorbitol, we observed more primary alcohols than secondary alcohols. No tertiary alcohols are formed in our reaction chemistry.

These dehydration reactions are most likely to occur over Brønsted acid sites. The presence of water also has a critical role in determining the rate of the dehydration reaction. In recent work of Iglesia et al. [44,45], it was found that the turnover rate for dehydration of 2-butanol increased with Brønsted acid strength; therefore, they suggested that the dehydration of 2-butanol can be used as a rigorous method to estimate the deprotonation energy (DPE) and acid strength for solid Brønsted acids. Dumesic et al. [46] also studied the catalytic performance of a series of solid acid catalysts for the dehydration 2-butanol with high water concentration. SiO₂-Al₂O₃, niobium phosphate and niobic acid were found to be stable and active for the dehydration of butanol. Their activities increased in the presence of water due to the increase in the concentration of Brønsted acid sites. Zeolites catalyst (Beta, USY, H-ZSM-5) and zirconia-based superacid catalysts (WO_x/ZrO₂ and MoO_x/ZrO₂) were ineffective due to deactivation or low catalytic activity. The lower activity of WO_x/ZrO₂ and MoO_x/ZrO₂ may be explained by their lower acidity in the presence of large amount of water.

4.4. Hydrogenation reactions

Hydrogenation occurs on the surface of active metal. Three different functionalities are hydrogenated in APHDO of sorbitol including: C=O bonds, C=C bonds, and C—O—C bonds. Only trace amounts of C=C bonds were detected which indicated that under our reactions conditions this reaction was fast. The only C=C bonds that were detected were in the furan form, which is more stable than straight chain C=C bonds. Only small amounts of C=O bonds were detected also indicating that this reaction is fast under our reaction conditions. However, large amounts of C—O—C bonds were detected. This indicates that the rate of hydrogenation increases for the different type of functionalities as C—O—C < C=O < C=C bonds. The C=O bonds may be present in higher concentrations on the metal surface. As discussed earlier, the C=O bonds are necessary for C—C bond cleavage. Therefore, it is desirable to find a metal catalyst that has a higher activity for both C=O bond and C=C hydrogenation if one wants to suppress C—C bond cleavage.

From the result mentioned earlier, we can see that both Brønsted acid site and metal sites are needed for production of alkanes. When a Pt catalyst is added to a support without Brønsted acid sites (such as carbon, alumina) [10,11], only a small amount of C5 and C6 alkanes are formed with CO₂, H₂ and light alkanes being the major product. In contrast, isosorbide is the final product when SiO₂-Al₂O₃ is the catalyst. At the same time, the cooperation of Pt and Brønsted acid sites (dehydration followed by hydrogenation) is very important for the high activity and selectivity of the catalyst towards larger alkanes. In the future, with the utilization of some new catalyst materials with strong Brønsted acidity (more

Brønsted acid sites, high acid strength, tolerance to poisoning) together with proper metals (or alloys) with higher activity for the hydrogenation reaction, we believe it will be possible to more selectively produce larger alkanes from sorbitol or other biomass-derived oxygenates.

4.5. Potential of hydrodeoxygenation routes to make targeted products

Biomass conversion involves oxygen removal [1]. Hydrodeoxygenation chemistry is one of the major critical routes to successfully remove oxygen from biomass-derived species and make targeted products liquid or oxygenated products. We have shown the chemistry of hydrodeoxygenation with sorbitol in this paper. This same chemistry can be applied to conversion of other biomass-derived species including bio-oils [47], C5 sugars, C6 sugars and even potentially lignin [16]. As we have shown in this paper, hydrodeoxygenation routes can produce a large variety of products including polyols, alcohols, ketones, cyclic ethers, and alkanes. Several other researchers have used hydrodeoxygenation chemistry to make targeted products including dimethylfuran [24], polyols [48], and tetrahydrofuran [49].

The products from hydrodeoxygenation pathways can be used for a variety of applications. Straight chain C5 and C6 alkanes could be isomerized into gasoline. Lighter alkanes can be used for natural gas or liquefied petroleum gas. Oxygenates and alkanes could also be used as gasoline or as chemicals. Targeted oxygenates can also undergo C—C bond formation reactions to produce diesel and jet fuel [13,14]. Short chain alcohols could be converted into olefins for polymer industry. Cyclic ethers can be separated and used as solvents, additives, or blending agents for transportation fuels [17]. Upgraded products can also be passed over zeolites catalysts to produce aromatics [17]. In this respect, APHDO is a critical reaction for conversion of biomass-derived species into targeted fuels and chemicals. However, it is necessary to understand and control the key fundamental reactions to use hydrodeoxygenation chemistry to make these targeted products. We project that with future understanding based on mechanistic insights into spectroscopic studies, theoretical study of catalyst surfaces and kinetic study improved APHDO processes will be developed which will allow us to more selectively make targeted products by hydrodeoxygenation chemistry.

5. Conclusions

In this work, we investigated the reaction pathways for the aqueous-phase hydrodeoxygenation (APHDO) of sorbitol over the 4 wt.% Pt/SiO₂-Al₂O₃ catalyst. A wide variety of reaction intermediates were identified by GC-MS and HPLC. From the analysis of the gas phase and liquid phase products from the APHDO of sorbitol and a series of model compounds, we can see that APHDO process is mainly composed of three classes of reactions: C—C bond cleavage, C—O bond cleavage, and hydrogenation reactions. The key C—C bond cleavage reactions include: retro-aldol condensation and decarbonylation which most likely occur on the surface of Pt metal. Dehydration is the most important C—O bond cleavage reaction and most likely occurs on Brønsted acid sites. Sorbitol initially undergoes either dehydration, to form 1,4-sorbitan and then isosorbide, or C—C retro-aldol condensation reactions to produce primarily C3 polyols. The isosorbide generated is converted to 1,2,6-hexanetriol by a ring opening hydrogenation step followed by dehydration/hydrogenation. The 1,2,6-hexanetriol is further dehydrated and hydrogenated to form hexane as the final product. Lighter alkanes and alcohols are produced by C—C bond cleavage decarbonylation reactions to form C1–C5 oxygenates and alkanes. It is likely that future advances in understanding the surface

chemistry of catalysts combined with improvements in design of catalysts and theoretical studies will allow us to use hydrodeoxygenation chemistry to make targeted products from biomass-derived species.

Acknowledgments

This work was supported by a NSF-MRI grant and by the Defense Advanced Research Project Agency through the Defense Science Office Cooperative Agreement W911NF-09-2-0010 (Surf-Cat: Catalysts for production of JP-8 range molecules from lignocellulosic Biomass. Approved for Public Release, Distribution Unlimited). We would like to thank T.P. Vispute, Dr. V.S. Ayyagari and H. Olcay for technical assistance.

References

- [1] G.W. Huber, S. Iborra, A. Corma, *Chem. Rev.* 106 (2006) 4044.
- [2] R.R. Davda, J.W. Shabaker, G.W. Huber, R.D. Cortright, J.A. Dumesic, *Appl. Catal. B – Environ.* 56 (2005) 171.
- [3] J.N. Chheda, G.W. Huber, J.A. Dumesic, *Angew. Chem. Int. Edit.* 46 (2007) 7164.
- [4] J.W. Shabaker, G.W. Huber, J.A. Dumesic, *J. Catal.* 222 (2004) 180.
- [5] J.W. Shabaker, R.R. Davda, G.W. Huber, R.D. Cortright, J.A. Dumesic, *J. Catal.* 215 (2003) 344.
- [6] G.W. Huber, J.W. Shabaker, S.T. Evans, J.A. Dumesic, *Appl. Catal. B: Environ.* 62 (2006) 226.
- [7] G.W. Huber, J.W. Shabaker, J.A. Dumesic, *Science* 300 (2003) 2075.
- [8] R.R. Davda, J.W. Shabaker, G.W. Huber, R.D. Cortright, J.A. Dumesic, *Appl. Catal. B: Environ.* 43 (2003) 13.
- [9] R.R. Davda, J.A. Dumesic, *Chem. Commun.* (2004) 36.
- [10] R.D. Cortright, R.R. Davda, J.A. Dumesic, *Nature* 418 (2002) 964.
- [11] G.W. Huber, R.D. Cortright, J.A. Dumesic, *Angew. Chem. Int. Edit.* 43 (2004) 1549.
- [12] Y.C. Lin, G.W. Huber, *Energy Environ. Sci.* 2 (2009) 68.
- [13] R.M. West, Z.Y. Liu, M. Peter, C.A. Gartner, J.A. Dumesic, *J. Mol. Catal. A – Chem.* 296 (2008) 18.
- [14] R.M. West, Z.Y. Liu, M. Peter, J.A. Dumesic, *ChemSusChem* 1 (2008) 417.
- [15] G.W. Huber, J.N. Chheda, C.J. Barrett, J.A. Dumesic, *Science* 308 (2005) 1446.
- [16] N. Yan, C. Zhao, P.J. Dyson, C. Wang, L.T. Liu, Y. Kou, *ChemSusChem* 1 (2008) 626.
- [17] E.L. Kunkes, D.A. Simonetti, R.M. West, J.C. Serrano-Ruiz, C.A. Gartner, J.A. Dumesic, *Science* 322 (2008) 417.
- [18] J.N. Chheda, J.A. Dumesic, *Catal. Today* 123 (2007) 59.
- [19] N. Ji, T. Zhang, M.Y. Zheng, A.Q. Wang, H. Wang, X.D. Wang, J.G.G. Chen, *Angew. Chem. Int. Edit.* 47 (2008) 8510.
- [20] A. Corma, G.W. Huber, L. Sauvinauda, P. O'Connor, *J. Catal.* 257 (2008) 163.
- [21] J.N. Chheda, Y. Roman-Leshkov, J.A. Dumesic, *Green Chem.* 9 (2007) 342.
- [22] Y. Roman-Leshkov, J.A. Dumesic, *Top. Catal.* 52 (2009) 297.
- [23] Y. Roman-Leshkov, J.N. Chheda, J.A. Dumesic, *Science* 312 (2006) 1933.
- [24] Y. Roman-Leshkov, C.J. Barrett, Z.Y. Liu, J.A. Dumesic, *Nature* 447 (2007) 982.
- [25] R.R. Davda, J.A. Dumesic, *Angew. Chem. Int. Edit.* 42 (2003) 4068.
- [26] E.P. Maris, R.J. Davis, *J. Catal.* 249 (2007) 328.
- [27] R. Alcalá, M. Mavrikakis, J.A. Dumesic, *J. Catal.* 218 (2003) 178.
- [28] E. Tronconi, N. Ferlazzo, P. Forzatti, I. Pasquon, B. Casale, L. Marini, A Mathematical-model for the Catalytic Hydrogenolysis of Carbohydrates, Pergamon-Elsevier Science Ltd., June 28–July 01, Turin, Italy, 1992, p. 2451.
- [29] D.K. Sohounloue, C. Montassier, J. Barbier, *React. Kinet. Catal. Lett.* 22 (1983) 391.
- [30] L. Zhao, J.H. Zhou, Z.J. Sui, X.G. Zhou, *Chem. Eng. Sci.* (2009), doi:10.1016/j.ces.2009.03.026.
- [31] B.W. Hoffer, R. Prochazka, WO 2008071642, BASF SE, Germany, 2008.
- [32] B.W. Hoffer, R. Prochazka, WO 2008071641, BASF SE, Germany, 2008.
- [33] B.W. Hoffer, R. Prochazka, WO 2008071616, BASF SE, Germany, 2008.
- [34] C. Cao, J.F. White, Y. Wang, J.G. Frye, *Chem. Ind.* 115 (2007) 289.
- [35] O. Munoz-Muniz, M. Quintanar-Audelo, E. Juaristi, *J. Org. Chem.* 68 (2003) 1622.
- [36] J. Binapfl, DE 875512, BAYER AG, 1953.
- [37] J.E. Dolfini, J. Glinka, S.C. Bosch, US Patent 4927805, 1990.
- [38] C.S. Cao, J.F. White, Y. Wang, J.G. Frye, in: S.R. Schmidt (Ed.), *Selective Hydrogenolysis of Sugar Alcohols Over Structured Catalysts*, CRC Press-Taylor & Francis Group, Orlando, FL, 2006, p. 289 (2–6 April).
- [39] I.T. Clark, *Ind. Eng. Chem.* 50 (1958) 1125.
- [40] I. Bucsi, Á. Molnár, M. Bartók, G.A. Olah, *Tetrahedron* 51 (1995) 3319.
- [41] M. Clugston, R. Flemming, *Advanced Chemistry*, Oxford University Press, 2000.
- [42] V.K. Ahluwalia, M. Goyal, *A Textbook of Organic Chemistry*, Alpha Science Int'l Ltd., 2000.
- [43] T. Nishiguchi, C. Kamio, *J. Chem. Soc. – Perkin Trans. 1* (1989) 707.
- [44] J. Macht, R.T. Carr, E. Iglesia, *J. Am. Chem. Soc.* 131 (2009) 6554.
- [45] J. Macht, R.T. Carr, E. Iglesia, *J. Catal.* 264 (2009) 54.
- [46] R.M. West, D.J. Braden, J.A. Dumesic, *J. Catal.* 262 (2009) 134.
- [47] T.P. Vispute, G.W. Huber, *Green Chem.* (2009), doi:10.1039/b912522c.
- [48] S. Koso, I. Furikado, A. Shimao, T. Miyazawa, K. Kunimori, K. Tomishige, *Chem. Commun.* (2009) 2035.
- [49] R.M. West, E.L. Kunkes, D.A. Simonetti, J.A. Dumesic, *Catal. Today* (2009), doi:10.1016/j.cattod.2009.02.004.